Advanced Robotics

ISSN: 0169-1864 (Print) 1568-5535 (Online) Journal homepage: https://www.tandfonline.com/loi/tadr20

Adaptive hybrid force/position control of robot manipulators using an adaptive force estimator in the presence of parametric uncertainty

Seyed Ali Mohamad Dehghan, Mohammad Danesh & Farid Sheikholeslam

To cite this article: Seyed Ali Mohamad Dehghan, Mohammad Danesh & Farid Sheikholeslam (2015) Adaptive hybrid force/position control of robot manipulators using an adaptive force estimator in the presence of parametric uncertainty, Advanced Robotics, 29:4, 209-223, DOI: 10.1080/01691864.2014.985609

To link to this article: https://doi.org/10.1080/01691864.2014.985609

Advanced Robotics, 2015
Vol. 29, No. 4, 209–223, http://dx.doi.org/10.1080/01691864.2014.985609

Taylor & Francis
Taylor & Francis Group

FULL PAPER

Adaptive hybrid force/position control of robot manipulators using an adaptive force estimator in the presence of parametric uncertainty

Seyed Ali Mohamad Dehghan[a]*, Mohammad Danesh[b] and Farid Sheikholeslam[a]

[a]*Department of Electrical and Computer Engineering, Isfahan University of Technology, 84156-83111 Isfahan, Iran;*
[b]*Department of Mechanical Engineering, Isfahan University of Technology, 84156-83111 Isfahan, Iran*

(*Received 18 November 2013; revised 30 May 2014 and 19 September 2014; accepted 16 October 2014*)

This study is devoted to sensorless adaptive force/position control of robot manipulators using a position-based adaptive force estimator (AFE) and a force-based adaptive environment compliance estimator. Unlike the other sensorless method in force control that uses disturbance observer and needs an accurate model of the manipulator, in this method, the unknown parameters of the robot can be estimated along with the force control. Even more, the environment compliance can be estimated simultaneously to achieve tracking force control. In fact, this study deals with three challenging problems: No force sensor is used, environment stiffness is unknown, and some parametric uncertainties exist in the robot model. A theorem offers control laws and updating laws for two control loops. In the inner loop, AFE estimates the exerted force, and then, the force control law in the outer loop modifies the desired trajectory of the manipulator for the adaptive tracking loop. Besides, an updating law updates the estimated compliance to provide an accurate tracking force control. Some experimental results of a PHANToM Premium robot are provided to validate the proposed scheme. In addition, some simulations are presented that verify the performance of the controller for different situations in interaction.

Keywords: sensorless force control; hybrid force/position control; adaptive force estimator; adaptive control; robot manipulators

1. Introduction

For execution of the robotic tasks requiring interaction with the environment, it is necessary to control the force exerted on the contact besides the position of the manipulator. When in contact, the end-effector position is constrained along certain directions by the environment, and it needs a suitable compliant behavior of the manipulator to facilitate the interaction.

The basic control strategy to exert the required force to the environment is stiffness control.[1] The proportional gain in the position control sets the robot's stiffness, which has to be properly tuned vs. environmental stiffness. Stiffness control is used to design a static interaction behavior. In order to achieve a desired dynamic behavior of the interaction, the mass and damping at the contact must be considered besides the stiffness, leading to impedance control.[2]

Another active compliance can be provided using hybrid position/force control,[3] where position and force are controlled in a non-conflicting way in two orthogonal subspaces.[4] Force control methods can be classified into explicit or implicit algorithms.[5] In explicit force control, the end-effector force is controlled by directly commanding the joint torques of the robot based on the force error.[6,7] In implicit force control, the end-effector force is controlled indirectly by modifying the reference trajectory of an inner loop joint position/velocity controller based on the force error.[8,9] The aim of the implicit hybrid control method is to implement force control on traditional position-controlled industrial manipulators. In [8], the authors presented an outer loop integral force control law, which provides asymptotically exact force set point regulation in the absence of inner loop velocity tracking errors. In fact, the control law provides bounded force errors in the presence of bounded inner loop velocity errors. In [9], the authors presented two implicit force controllers, which guarantee asymptotically exact force trajectory tracking under exact or asymptotically exact inner loop velocity control. Actually, they estimate the compliance of environment for force tracking control. In [5], different force control methods were reviewed and their advantages and drawbacks were discussed.

Mounting force sensors on the end effector for sensing this force was the only way for years, which led to the high cost of price, repairs, and maintenance. High noise, soft structure, limited directions of sensing and increased complexity are the other drawbacks of using force sensors.[10–13] Recent advances in processors enable researchers to develop control algorithms and eliminate some instruments and consequently simplify

*Corresponding author. Email: sam.dehghan@eng.ui.ac.ir

the overall mechanism and reduce the cost. A common method to eliminate force sensors is employing disturbance observers. In the last two decades, many researches focused on disturbance observers and developed them in many applications.[10–15] Some researchers used these observers for torque or force sensing and control.[11–13] In [12], the authors studied the validation of disturbance observers for force control of a 6-DOF manipulator and compared the results with that of force control with force sensors. In [16], the authors analyzed the stability of a disturbance observer with variations of inertia. The majority of these observers are designed based on linear systems. Therefore, compensating all nonlinearities before using them is required. Consequently, some researchers presented nonlinear-based designs of the disturbance observer.[17–19] However, they need an accurate model of friction and robot dynamics too. [13] and [20] estimated robot dynamics in different phase with no contact forces and finally used disturbance observer with the identified accurate model to control the contact force. In [21], time delay estimation is used to estimate the nonlinear dynamic of the manipulator in which the modeling process is in non-contact operation. Although disturbance observers are completely efficient in estimating the external force as disturbance, they have weaknesses in dealing with the uncertainties.[13,22] In [23], a simple force estimator method is reviewed that uses the position error of the manipulator to estimate the force, which can be weakly used for accurate force control.

Adaptive control is another approach for facing the disturbances and uncertainties that many researchers used for motion control criteria.[24–26] Consequently, there are some studies to estimate the external force using adaptive approaches. Another disturbance estimator procedure is position-based adaptive disturbance estimator. In [27], authors used a combination of an extended Kalman filter to estimate states and an adaptive law to estimate the force in position control of the manipulator. In [28], the authors proposed an adaptive disturbing force rejection through the position tracking control. That approach compensates disturbing force using a position-based adaptive law that updates the estimated force of the control law. There is no need to compute the inverse of Jacobian transpose; hence, the controller works efficiently close to singular points. The force rejection approach was expanded in [29] to estimate and reject disturbing force and parametric uncertainty simultaneously. However, these force estimators have not yet been used for force control and are used just for force effect rejection through position control.

This study uses an implicit force control where an adaptive force estimator (AFE) is used to estimate and control the desired force. For this purpose, a two-loop control architecture is proposed. First, an adaptive position control is used to track the trajectory and estimate the force and the parametric uncertainty in the inner loop, and then, an outer adaptive force control loop is used to modify the trajectory of the manipulator in the force-controlled directions and estimate the environment compliance. The asymptotical stability of the system is guaranteed due to the Lyapunov-based design methodology. An additional condition specifies the ability of AFE in force estimation. This approach shows no weaknesses against parametric uncertainty and other modeled nonlinearities such as frictions. Since the position of the environment is not known, it is inevitable that the robot will work in non-contact operation while the force is commanded. Here, a brief study is done for non-contact operation of the robot with the proposed adaptive force controller. The main contributions of this study can be expressed as follows:

(1) This study gives a novel capability to sensorless force control schemes to deal with the parametric uncertainty in the robot model.
(2) Unlike some of the other sensorless force control schemes, this procedure does not need Jacobian inverse in its force computations.
(3) This study acquires the force tracking control by estimating the environment compliance (stiffness) without using force sensor. Note that this was done for sensor-based approaches before.

Some experimental and simulation results validate the efficiency of the proposed hybrid position/force controller. Finally, some discussion about the bandwidth of the force estimator is presented to check the capability of the controller in dealing with different environments.

The remainder of this study is organized as follows. The next section describes robot and environment modeling. Third section explains the proposed controller design and represents a theorem for analysis of contact operation of the manipulator. Fourth section includes some experimental results of a PHANToM Premium robot. Fifth section demonstrates the results of some simulation studies for a manipulator interacting with the environment in different conditions. Finally, the sixth section contains the study conclusions.

2. System model

Consider dynamic equations of an n-joint rigid robot manipulator described by

$$M(q)\ddot{q} + C(q,\dot{q})\dot{q} + G(q) + B(\dot{q}) + J(q)^T F = \tau \quad (1)$$

where $q \in \mathcal{R}^n$ is the vector of joint position, $M(q) \in \mathcal{R}^{n\times n}$ is the symmetric positive definite inertia matrix, $C(q,\dot{q}) \in \mathcal{R}^{n\times n}$ is the Coriolis and centrifugal forces matrix, $G(q) \in \mathcal{R}^n$ is the vector of gravity

torques, $B(\dot{q}) \in \mathcal{R}^n$ is the vector of friction, $\tau \in \mathcal{R}^n$ is the vector of input joint torques (control input), $F \in \mathcal{R}^m$ is the external force vector exerted on the environment, and $J(q) \in \mathcal{R}^{m \times n}$ is the Jacobian matrix. Based on the linear parameterization property of robots dynamic, motion equations can be expressed by

$$M(q)\ddot{q} + C(q,\dot{q})\dot{q} + G(q) + B(\dot{q}) = Y(q,\dot{q},\ddot{q})\varphi \quad (2)$$

where $Y(q,\dot{q},\ddot{q})$ is the regression matrix and φ is the parameter vector.

Assume that the environment can be modeled as a linear spring with a known stiffness K_e. In this system, if the position of the manipulator is greater than the environment boundary in each direction, the force exerted on the environment is given by

$$F_N = K_{eN}(p_N - p_{eN}) \quad (3)$$

where p_{eN} and $p_N \in \mathcal{R}^m$ are the environment boundary and the end-effector position in the force-controlled directions of the task space, respectively. Actually, N is a subspace containing the corresponding force-controlled directions. Here, index T shows the position-controlled directions and index N shows the force-controlled directions. Therefore, vectors and diagonal matrices can be decomposed into two non-conflicting directions as follows:

$$\Omega = \Omega_N + \Omega_T, \quad \text{for} \quad \Omega \in \mathcal{R}^{n \times n} \quad \text{or} \quad \Omega \in \mathcal{R}^{n \times 1} \quad (4)$$

where $\Omega_N = N\Omega$ and $\Omega_T = T\Omega$. Now, define compliance of the environment as Ξ_N and therefore (3) can be written as

$$\Xi_N F_N = p_N - p_{eN}$$

where $\Xi_N = (K_{eN} + T)^{-1} - T$. Also in this study, Ω^i means the ith element of the vector $\Omega \in \mathcal{R}^{n \times 1}$ or the ith element of the main diagonal of the matrix $\Omega \in \mathcal{R}^{n \times n}$.

3. Controller design

Assume a manipulator with inaccurate model parameters that an unknown external force is exerted on it. For proper control of the manipulator using model-based algorithms, parameters and external force must be determined accurately as much as possible. Actual position and desired trajectory of the end effector in the task space are expressed by p and p_d, respectively. p_d can be decomposed into two complementary subspaces as $p_d = p_{dN} + p_{dT}$. Define the tracking error as $e_p = p_d - p$ and two auxiliary signals as $\dot{q}_r = J^{\dagger}(\Lambda e_p + \dot{p}_d)$ and $S_p = \Lambda e_p + \dot{e}_p$, where Λ is a positive definite diagonal matrix and $J^{\dagger}$ is pseudoinverse of the Jacobian [30]. Then, we have $S = \dot{q}_r - \dot{q}$ in joint space. Based on linear parameterization of robot motion equations, one can write for any $\dot{q}_r$

$$M(q)\ddot{q}_r + C(q,\dot{q})\dot{q}_r + G(q) + B(\dot{q}) = Y(q,\dot{q},\dot{q}_r,\ddot{q}_r)\varphi \quad (5)$$

where φ was mentioned in (2). Now, define the estimations of φ and F as $\hat{\varphi}$ and $\hat{F}$, respectively; then, the estimation errors are $\tilde{\varphi} = \varphi - \hat{\varphi}$ and $\tilde{F} = F - \hat{F}$.

Figure 1 illustrates the proposed scheme for sensorless force control. This figure shows two main loops; the first one is the AFE loop and the outer one is the adaptive force control loop. The estimated force is fed to the force controller instead of the real force, and this constructs the outer loop feedback. The adaptive force controller estimates the environment compliance and defines the trajectory of the robot in the force-controlled directions. In the following, a theorem presents the force control law for a manipulator in contact with an environment using an AFE that guarantees the whole system stability through some conditions. Before representing the theorem, a lemma is introduced that is used in proofs.

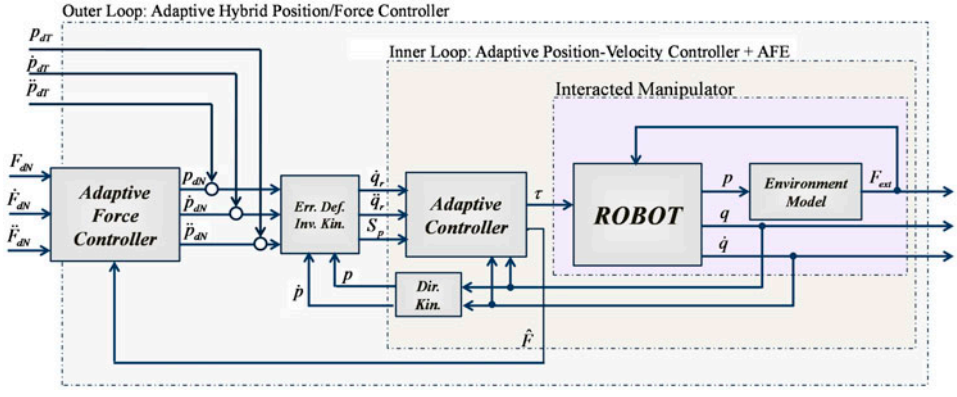

Figure 1. Block diagram of the proposed AFE-based adaptive hybrid position/force control scheme.

Lemma *Consider* $A(t)X \equiv 0$, *where* $A(t) \in \mathcal{R}^{k\times l}$ *and* $X \in \mathcal{R}^{l}$. *It can be derived that* $X \equiv 0$ *for* $[t_0, t_0 + t]$ *if there exist two positive constants* α_1 *and* α_2 *such that*

$$\alpha_1 I \leq \int_{t_0}^{t_0+t} A(t)^T A(t)dt \leq \alpha_2 I, \quad \forall\ t_0 \geq 0 \tag{6}$$

Proof It can be derived that $X \equiv 0$ if $A(t)$ is full column rank. This needs $Q = \int_{t_0}^{t_0+t} A(t)^T A(t)dt$ to be a non-singular or positive definite matrix.[31] Using the Rayleigh–Ritz theorem,[25] we can write (6) for this positive definite Q.

Theorem 1 *Consider the control system of Figure 1 with the robot dynamic* (1) *interacted with the environment* (3) *and the control laws*

$$\tau = Y(.)\hat{\varphi} + K_V S + J^T(\hat{F} + K_p S_p) \tag{7}$$

$$\dot{p}_{dN} = \hat{\Xi}_N \dot{F}_{dN} + K_F e_{FN} \tag{8}$$

and the updating laws

$$\dot{\hat{\varphi}} = \Gamma_\varphi Y^T(.)S \tag{9}$$

$$\dot{\hat{F}} = -\Gamma_F S_P \tag{10}$$

$$\dot{\hat{\Xi}}_N = \Gamma_\Xi e_{FN} \dot{F}_{dN}^T \tag{11}$$

where Γ_φ, Γ_F, K_V, K_p, K_F, *and* Γ_Ξ *are diagonal positive definite matrices and* $e_{FN} = F_{dN} - \hat{F}_N$ *is the force error. If* $A(q_d(t)) = [Y(.), J^T(.)]$ *satisfies the condition* (6) *and elements of* K_p *are selected enough large to satisfy,*

$$K_p^i > \max\Big((1 + \bar{\Xi}_N^i \Gamma_F^i)^2, (\bar{\Xi}_N^i \Gamma_F^i)^2 \Lambda^i\Big)/K_F^i, \quad i \in \{N\} \tag{12}$$

where $\bar{\Xi}_N^i$ *is the maximum possible compliance of the environment in the corresponding direction; then, the closed loop system is stable and tracking errors of force and position converge to zero asymptotically. In addition, for* $\dot{F}_{dN}^i \neq 0, \quad i \in \{N\}$, *compliance estimation converges to its real value and this yields the asymptotic stability of the whole system.*

Proof

Substituting the control law (7) into (1) yields

$$M\dot{S} = Y\tilde{\varphi} - CS - K_V S + J^T\tilde{F} - J^T K_p S_p \tag{13}$$

Consider the parameters and external force to be constants; thus, $\dot{\tilde{\varphi}} = -\dot{\hat{\varphi}}$ and $\dot{\tilde{F}} \simeq -\dot{\hat{F}}$. Using $\dot{F}_N = K_{eN}\dot{p}_N$ and substituting (10) and (8) into the derivative of $e_{Fi} = F_{di} - F_i + \tilde{F}_i$ gives

$$\dot{e}_{FN} = -K_{eN}\dot{p}_N + \dot{\tilde{F}}_N = -K_{eN}K_F e_{FN} + K_{eN}\dot{e}_{pN} + \Gamma_F S_{pN} \tag{14}$$

Now, converting the stiffness to compliance yields

$$\Xi_N \dot{e}_{FN} = \tilde{\Xi}_N \dot{F}_{dN} - K_F e_{FN} + \dot{e}_{pN} + \Xi_N \Gamma_F S_{pN} \tag{15}$$

Considering (13), (15), S, and updating laws, the closed loop system states can be selected as $S, e_p, \tilde{\varphi}, \tilde{F}$ and e_{Fi}. Now, let the candidate Lyapunov function be

$$V_s = \frac{1}{2}S^T M S + e_p^T \Lambda K_p e_p + \frac{1}{2}\tilde{\varphi}^T \Gamma_\varphi^{-1}\tilde{\varphi} + \frac{1}{2}\tilde{F}^T\Gamma_F^{-1}\tilde{F} + \frac{1}{2}e_{FN}^T K_{eN}^{-1} e_{FN} + \frac{1}{2}\text{trace}(\tilde{\Xi}_N^T \Gamma_\Xi^{-1}\tilde{\Xi}_N) \tag{16}$$

Differentiating (16) yields

$$\dot{V}_s = S^T M\dot{S} + \frac{1}{2}S^T\dot{M}S + 2\dot{e}_p^T\Lambda K_p e_p + \dot{\tilde{\varphi}}^T\Gamma_\varphi^{-1}\tilde{\varphi} + \dot{\tilde{F}}^T\Gamma_F^{-1}\tilde{F} + \dot{e}_{FN}^T K_{eN}^{-1} e_{FN} + \text{trace}(\dot{\tilde{\Xi}}_N^T\Gamma_\Xi^{-1}\dot{\tilde{\Xi}}_N) \tag{17}$$

Substituting (13) and (14) into (17) and simplifying the equations gives

$$\begin{aligned}\dot{V}_s = {} & \frac{1}{2}S^T(\dot{M} - 2C)S - S^T K_V S - S_p^T K_p S_p + 2\dot{e}_p^T\Lambda K_p e_p \\ & + \Big(S^T Y\tilde{\varphi} + \dot{\tilde{\varphi}}^T{}_\varphi{}^{-1}\tilde{\varphi}\Big) + \Big(S^T J^T\tilde{F} + \dot{\tilde{F}}^T\Gamma_F^{-1}\tilde{F}\Big) \\ & + \big(-K_F e_{FN} + \dot{e}_{pN} + \Xi_N\Gamma_{FN}S_{pN}\big)^T e_{FN} + \dot{F}_{dN}^T\tilde{\Xi}_N^T e_{FN} \\ & + \text{trace}(\tilde{\Xi}_N^T\Gamma_\Xi{}^{-1}\dot{\tilde{\Xi}}_N)\end{aligned} \tag{18}$$

Skew-symmetry property of $(\dot{M} - 2C)$ results in $S^T(\dot{M} - 2C)S = 0$. Using (9)-(10) and $\dot{F}_{dN}^T\tilde{\Xi}_N^T e_{FN} = \text{trace}(\tilde{\Xi}_N^T e_{FN}\dot{F}_{dN}^T)$, (18) can be rewritten as

$$\begin{aligned}\dot{V}_s = {} & -S^T K_V S - S_p^T K_p S_p + 2\dot{e}_p^T\Lambda K_V e_p - e_{FN}^T K_F e_{FN} \\ & + \dot{e}_{pN}^T e_{FN} + S_{pN}^T\Gamma_F\tilde{\Xi}_N e_{FN}\end{aligned} \tag{19}$$

and expanding S yields

$$\begin{aligned}\dot{V}_s = {} & -S^T K_V S - \dot{e}_p^T K_p\dot{e}_p - e_p^T\Lambda K_p e_p - e_{FN}^T K_F e_{FN} \\ & + \dot{e}_{pN}^T(N + \Gamma_F K_{eN}^{-1})e_{FN} + e_{pN}^T\Lambda\Gamma_F K_{eN}^{-1}e_{FN} \\ = {} & -S^T K_V S - \dot{e}_p^T D\dot{e}_p - e_p^T\Lambda B e_p - e_{FN}^T H e_{FN} \\ & - QQ^T - RR^T\end{aligned} \tag{20}$$

where D, B, H, Q, and R are as follows:

$$D_T = K_{pT}, \quad D_N = K_{pN} - \frac{1}{\alpha^2}(N + \Gamma_{FN}K_{eN}^{-1})^2$$

$$B_T = K_{pT}, \quad B_N = K_{pN} - \frac{1}{\alpha^2}(\Gamma_{FN}K_{eN}^{-1})^2\Lambda_N$$

$$H = K_{FN} - 2\alpha^2 I$$

$$Q = \frac{1}{\alpha}\dot{e}_{pN}^T(N + \Gamma_{FN}K_{eN}^{-1}) - \alpha e_{FN}$$

$$R = \frac{1}{\alpha}e_{pN}^T\Lambda_N\Gamma_{FN}K_{eN}^{-1} - \alpha e_{FN} \tag{21}$$

and α is a positive constant. Then, (20) can be written as

$$\dot{V}_s \leq -S^T K_V S - \dot{e}_p^T A\dot{e}_p - e_p^T\Lambda B e_p - e_{FN}^T H e_{FN} \tag{22}$$

Here, if the controller gains are selected so that D, B, and H remain positive definite, then, $\dot{V}_s \leq 0$ and since V_s is positive definite and radially unbounded, based on the Lyapunov direct method, the whole system is uniformly stable. Hence, if the initial conditions of states are bounded, all of the states $S, e_p, \tilde{\varphi}, \tilde{F}$ and e_{FN} remain bounded. Moreover, based on the Barbalat lemma, $\dot{V}_s \to 0$ as $t \to \infty$, since V_s is lower bounded and $\dot{V}_s$ is negative semi-definite and uniformly continuous in time. This indicates that $\left[S^T, \dot{e}_p^T, e_p^T, e_{FN}^T\right]^T \to 0$ as $t \to \infty$. Moreover, for $t \to \infty$, derivatives of e_{Fi} and S converge to zero. Thus, it can be derived from (15) that $\tilde{\Xi}_N \to 0$ for non-zero $\dot{F}_{dN}$ and (13) can be written as

$$\lim_{t\to\infty}\left[\, Y(q_d, \dot{q}_d, \ddot{q}_d) \quad J^T(q_d)\,\right]\begin{bmatrix}\tilde{\varphi}\\ \tilde{F}\end{bmatrix} = 0 \tag{23}$$

On the other hand, if A satisfies (6), it implies that $\lim_{t\to\infty}\left[\,\tilde{\varphi} \quad \tilde{F}\,\right]^T = 0$. This means that the errors of estimated parameter and force vectors converge to zero, and this intends the asymptotic stability of the system. Defining $E_{FN} = F_{dN} - F_N = e_{FN} - \tilde{F}_N$ and considering the asymptotic convergence of e_{FN} and $\tilde{F}$ to zero yields asymptotic convergence of E_{FN} to zero. Note that the sufficient condition to satisfy the positive definiteness of A, B, and H is selecting suitable gains that satisfies the following conditions:

$$\left.\begin{array}{c} H^i > 0 \Rightarrow \frac{K_F^i}{2} > \alpha^2 \\ D_N^i > 0 \Rightarrow \alpha^2 > \frac{1}{K_p^i}(1 + \Xi_N^i\Gamma_F^i)^2 \\ B_N^i > 0 \Rightarrow \alpha^2 > \frac{1}{K_p^i}(\bar{\Xi}_N^i\Gamma_F^i)^2\Lambda^i \end{array}\right\} i \in \{N\} \tag{24}$$

These conditions can be simplified as

$$K_p^i > \max\left(\left(1 + \bar{\Xi}_N^i\Gamma_F^i\right)^2, \left(\bar{\Xi}_N^i\Gamma_F^i\right)^2\Lambda^i\right)/K_F^i, \quad i \in \{N\} \tag{25}$$

where $\bar{\Xi}_N^i$ is an approximation of possible maximum compliance of the environment in the nth direction of the task space. This condition can be easily satisfied by choosing suitable gains. In fact, this condition is a sufficient condition, not a necessary one. That means if K_p^i is not enough large, then may $(J^{-T}K_V J^{-1})^i$ do its job.

□

The presented theorem shows the stability of the force control system for a manipulator in contact with the environment. Actually, measuring the accurate position of the environment boundary is not easily possible. Therefore, the environment position is assumed unknown in the literature.[7,12,32] Now, assume that the robot is not interacting with the environment. What will happen if a desired force is commanded in one or more directions? Here, a brief study on the performance of the control system for the manipulator in non-contact operation is presented.

If the manipulator is not interacting with the environment, $\dot{F}_N = K_{eN}\dot{p}_N$ is not established and e_{FN} is modified as

$$e_{FN} = F_{dN} - \hat{F}_N = F_{dN} + \tilde{F}_N \tag{26}$$

Thus, e_{FN} is not state of the system, and the inner loop system states can be considered as $S, e_p, \tilde{\varphi}$ and $\tilde{F}$. To analyze the inner loop stability, a method similar to that of in theorem1 can be used. Consider the candidate Lyapunov function

$$V_s = \frac{1}{2}S^T M S + e_p^T\Lambda K_p e_p + \frac{1}{2}\tilde{\varphi}^T\Gamma_\varphi^{-1}\tilde{\varphi} + \frac{1}{2}\tilde{F}^T\Gamma_F^{-1}\tilde{F} \tag{27}$$

Differentiating (27) and substituting (9)–(10) and (13) into it yields

$$\dot{V}_s = -S^T K_V S - \dot{e}_p^T K_p\dot{e}_p - e_p^T\Lambda K_p e_p \tag{28}$$

It means that tracking errors converge to zero; thus, if A (.) satisfies (6), then the estimation errors converge to zero too. Now, for analyzing the outer loop, define $E_{pN} = p_{eN} - p_N$ as the distance between the end effector and the environment boundary. Substituting (8) into $\dot{E}_{pN} = -\dot{p}_N$ and using the fact that $F_i = 0$ yields

$$\begin{aligned}\dot{E}_{pN} &= -\dot{p}_{dN} + \dot{e}_{pN} = -\hat{\Xi}_N\dot{F}_{dN} - K_F(F_{dN} - \hat{F}_N) + \dot{e}_{pN}\\ &= K_F F_{dN} + K_F\tilde{F}_N + \dot{e}_{pN}\end{aligned} \tag{29}$$

It can be written as

$$\dot{E}_{pN} + K_F F_{dN} + \hat{\Xi}_N\dot{F}_{dN} = u(t) \tag{30}$$

where $u(t) = K_F\tilde{F}_N + \dot{e}_{pN}$. Thus, (30) is a differential equation, and considering the same signs of corresponding elements in F_{dN} and E_{pN}, the unforced system is stable if every element of $K_F F_{dN}$ be larger than the corresponding element of $\hat{\Xi}_N\dot{F}_{dN}$. In fact, this condition would be satisfied since $\hat{\Xi}$ remains in a limited value around actual compliance, which decreases the effect of $\dot{F}_{dN}$ in (30). Additionally, $\hat{\Xi}_N$ is the other state of the outer loop system that should be analyzed. To do this, consider (11) that each element of F_{dN} is a bounded signal and each element of $\dot{F}_{dN}$ is a zero-mean signal. Since

the period of the desired force is limited, $\hat{\Xi}_N$ would vary in a limited bound around its initial value. Thus, K_F^i can be easily selected enough large to stabilize (30). Now, consider the stability of the inner loop and convergence of $u(t)$ to zero, then, the convergence of end effector to the environment can be achieved. Consequently, tracking errors of the position-controlled directions converge to zero, and the end effector reaches to the environment in the force-controlled directions.

Another property of a force estimator that is important for force control applications is its estimation bandwidth. Since the proposed AFE is nonlinear and time varying, its analysis is more complicated. First, we compute the relation between the real and the estimated force independently. For this, assume that the robot parameters are accurately estimated and then use (10) and its derivative to substitute in (13) to have

$$MJ^{-1}(\ddot{\hat{F}} - \Gamma\dot{J}J^{-1}\Gamma^{-1}\dot{\hat{F}}) = -(C + K_V)J^{-1}\Gamma^{-1}\dot{\hat{F}} + J^T F - J^T\hat{F} - J^T K_p\Gamma^{-1}\dot{\hat{F}} \tag{31}$$

Now, if it is assumed that the robot is fixed which means that $M(q)$, $J(q)$ and $C(q,\dot{q})$ are not time varying, then, this equation can be used to obtain the transfer function of the force estimation, which is

$$\hat{F}(s) = (Is^2 + \beta s + \alpha)^{-1}\alpha F(s) \tag{32}$$

where α and β are computed locally for the robot in its current position.

$$\alpha = JM^{-1}J^T\big|_{q=q_0}, \quad \beta = \big[JM^{-1}\big(J^T K_p + (C + K_V)J^{-1} - MJ^{-1}\dot{J}J^{-1}\big)\Gamma^{-1}\big]\big|_{q=q_0,\dot{q}=0} \tag{33}$$

Existence of Jacobian matrix in this system shows that the best performance of this estimator is when the robot works enough far from its singular points. It also shows that the natural frequency of the system is related to the Jacobian and the inverse of inertia matrices of the robot. However, the parameters K_I, K_p, and Γ can be changed to adjust the damping coefficient of the system.

Remark 1 Checking the condition (6) may not be easily possible. Instead, some considerations can be used during the design. Some of these considerations are as follows:

(1) Reducing the unknown parameters helps increasing the excitation of the system. Thus, adapt any parameters of robot that are not changing during the operation before interaction and just update those parameters that may change during the operation, such as the last link mass or inertia as it may carry loads.

(2) It seems that when $A(.)$ is a square matrix, then it satisfies (6) except in its singular points. Thus, for convergence assurance, the number of adaptive parameters can be selected less or equal to the robot joints.

Note that the considerations in Remark 1 are just to provide an apparent assurance of exact force estimation without checking (6). This means that condition (6) can be hold even if none of the considerations is satisfied. In worst case, if the force estimation is not accurate, we can adapt all the parameters or the specific parameters that are making troubles for the force estimation before using the AFE. In these cases, the procedure is apparently similar to disturbance observer in which the exact dynamic must be identified with this exception that the Jacobian inverse is not required anymore.

4. Experimental results

For validating the proposed AFE-based force control scheme, a PHANToM Premium robot (Sensable Technologies Inc., MA, USA) is selected as the force-controlled manipulator with a JR3 force sensor (JR3, Inc., Woodland, CAN) mounted on its end effector for validating the force control scheme. The utilized PHANToM device is a three degree-of-freedom robot that maps the generalized joint angles of the robot to the Cartesian position, which is shown in Figure 2. The dynamic model proposed in [33] is used to define the main parameters and compute the parameters' regressor. The third joint is fixed at zero, and the simplified dynamic is used to define the parameters' vector as follows:

$$\boldsymbol{\varphi} = [\varphi_1, \varphi_2, \varphi_3, \varphi_4]^T$$

$$\varphi_1 = \frac{1}{2}\big(I_{ayy} + I_{azz} + 2I_{baseyy} + I_{beyy} + I_{bezz} + I_{cyy} + I_{czz} + I_{dfyy} + I_{dfzz} + l_1^2 m_a + \frac{1}{4}l_2^2 m_a + \frac{1}{4}l_1^2 m_c + l_3^2 m_c\big)$$

$$\varphi_2 = \left(I_{bexx} + I_{cxx} + l_1^2 m_a + \frac{1}{4}l_1^2 m_c\right)$$

$$\varphi_3 = \frac{1}{2}\left(I_{beyy} - I_{bezz} + I_{cyy} - I_{czz} + l_1^2 m_a + \frac{1}{2}l_1^2 m_c\right)$$

$$\varphi_4 = g\left(\frac{1}{2}l_2 m_a + l_3 m_c - l_6 m_{df}\right) \tag{34}$$

For more information about the parameters definitions, please refer to [33]. In this experiment, these main four parameters are unknown.

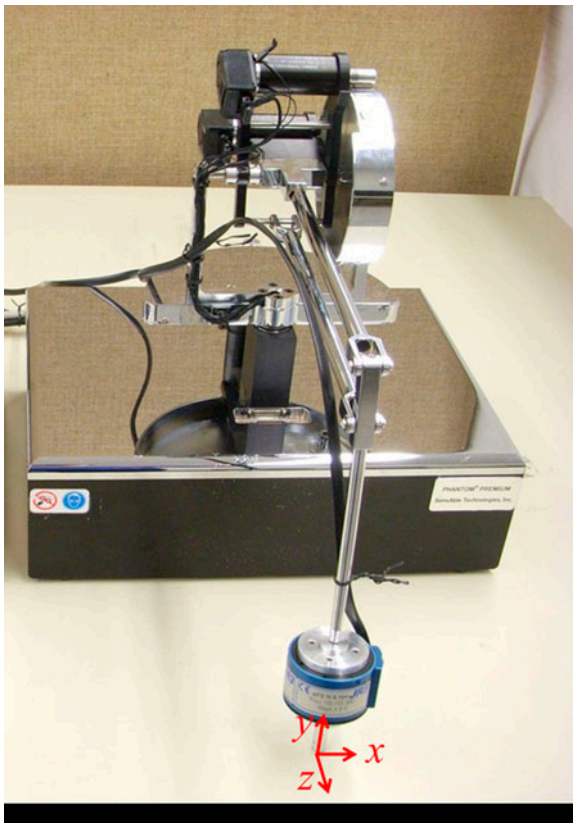

Figure 2. Experimental platform, PHANToM Premium robot (Sensable Technologies Inc., MA, USA), with a JR3 force sensor (JR3, Inc., Woodland, CAN).

Furthermore, the robot end effector is connected to a spring in direction y, where its stiffness is approximately 150 N/m. Position control of the robot in direction x and its force regulation control in direction y are the main goals of this experiment.

The desired force is selected as $F_d = 2$ N. The controller parameters are chosen as $\Lambda = 15I$, $K_V = 0.3I$, $K_p = 0.1I$, $\Gamma_\phi = \mathrm{diag}\left([10^{-3}, 10^{-3}, 10^{-2}, 10^{-2}]\right)$, $\Gamma_F = 10^3$, and $K_F = 1$. Since the desired force is a constant force, there is no need to estimate the environment, and thus, $\Gamma_\Xi = 0$. The initial values of the estimated parameters are $\boldsymbol{\varphi}(0) = 10^{-3}[2.4, 1.132, 2.4, 16.28]^T$. Figure 3 illustrates the results of this experiment. As it is shown in this figure, the tracking control is done toward x-axis while the force exerted on y-axis is regulated. The estimated parameters have initial changes that affect both velocity of the robot and the estimated force. However, next to their convergences, the force control performance improves effectively. Indeed, Figure 3 clearly shows the effect of unmodeled uncertainties in position tracking control and also in force regulation. The inevitable errors of speed trajectory and the regulated force in each cycle are because of some unmodeled uncertainties such as static friction of joints (the kinetic one is modeled and compensated through the dynamic model) and joint elasticity. To see the bandwidth of the force control procedure in this experiment, an equivalent frequency response of the force is obtained from force step response in Figure 3, which is depicted in Figure 4. The bandwidth for this experiment is 11 (1.75 Hz), which is affected by de-noising filtering delay and limited bandwidth, some parametric uncertainty in the model at the beginning and other inevitable unmodeled uncertainties like joint elasticity in the robot.

5. Simulation results

In addition to experimental study of the proposed approach, some simulation results are provided to check out the efficiency of the proposed approach more accurately. These simulations are for force tracking control of the robot while there are parametric uncertainties in the robot and the environment models. Moreover, the interactions of the robot with two highly different environments are studied.

The simulated robot is a SCARA manipulator without considering the third prismatic link shown in Figure 5. The used model is

$$M(q) = \begin{bmatrix} (m_1+m_2)l_1^2 + m_2 l_2^2 + 2m_2 l_1 l_2 c_2 & m_2 l_2^2 + m_2 l_1 l_2 c_2 \\ m_2 l_2^2 + m_2 l_1 l_2 c_2 & m_2 l_2^2 \end{bmatrix}$$
$$C(q,\dot{q}) = \begin{bmatrix} -m_2 l_1 l_2 (2\dot{q}_1\dot{q}_2 + \dot{q}_2^2) s_2 \\ m_2 l_1 l_2 s_2 \end{bmatrix}, s_2 = \sin(q_2), c_2 = \cos(q_2) \tag{35}$$

Parameters of the robot are $l_1 = l_2 = 1$ m, $m_1 = 2.3$ kg, and $m_2 = 0.8$ kg. In the simulation process, the Runge–Kutta integration method with the time step of 1 ms is used. Following simulations demonstrate the performance of the force control procedure. In all cases, the controlled force is in x-axis direction and the boundary of the environment is $x_e = 0.8$ m in this direction. Considering the environment position in robot task space, the estimated force is limited to positive values. In addition, it is assumed that the second link mass is not known exactly. Actually, other parameters can be adjusted in non-contact operations,[13,20,21] but the second link mass may vary over different operations. The initial values for the estimated mass and compliance are selected as $\hat{m}_2(0) = 0.5\,\mathrm{kg}$ and $\hat{\Xi}(0) = 0\,\mathrm{m/N}$ in all cases. $F_{dx} = 10 + 5\sin(3t)$ N is the desired force, and $p_{dy} = 0.1 + 0.2\sin(2t)$ m is the desired trajectory of the manipulator in x-axis and y-axis, respectively. In addition, initial position of the robot is selected as $p(0) = [0.75 \quad 0.28]^T$.

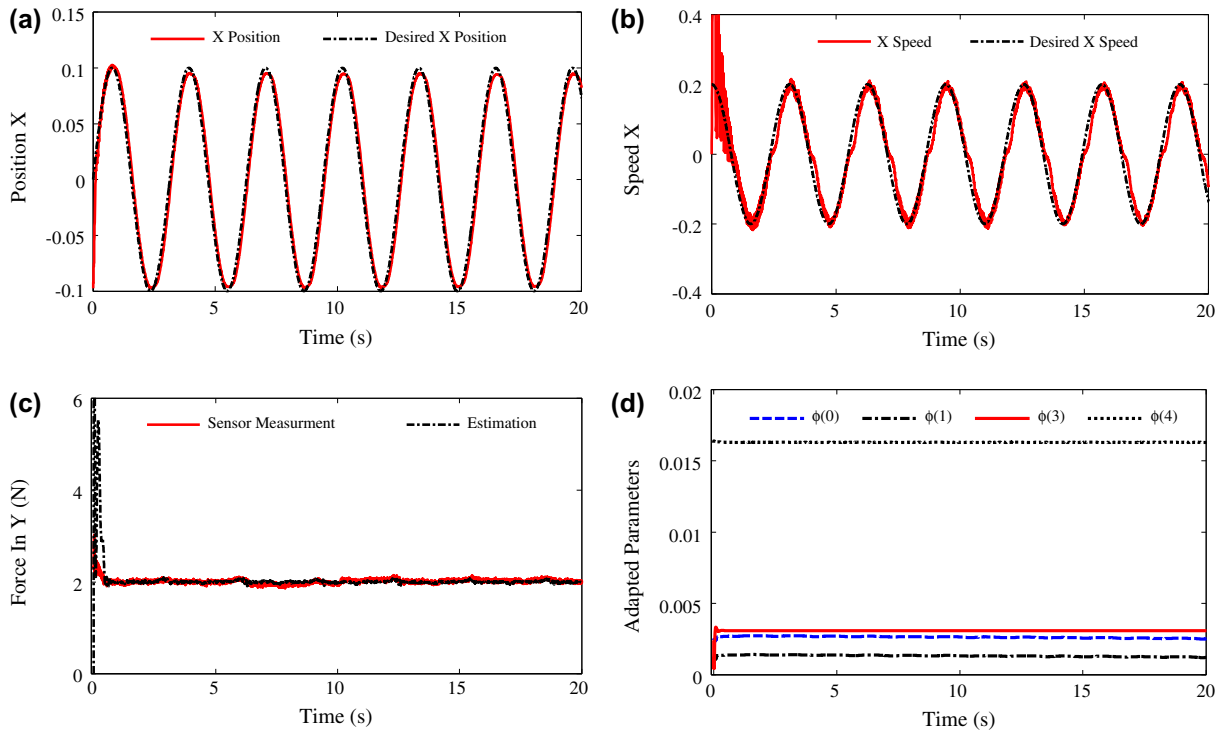

Figure 3. Experimental force control results, (a) end-effector position tracking in x-axis, (b) end-effector speed tracking in x-axis, (c) force control result in y-axis: estimated and sensor measured force of the end effector, and (d) estimated parameters of the robot.

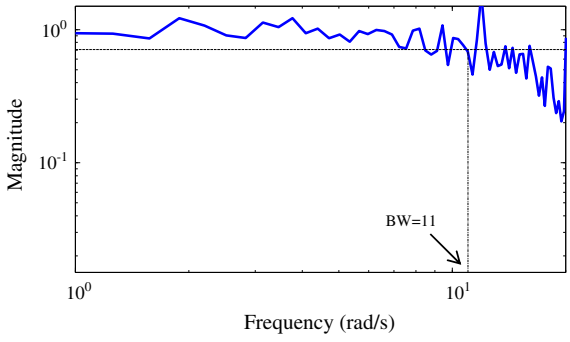

Figure 4. The frequency response of the force control experiment.

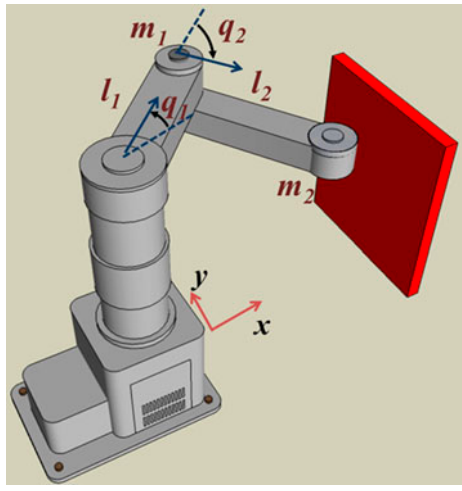

Figure 5. The simulated manipulator; the robot has force tracking in direction x and position tracking in direction y.

Simulation 1. In first case, a low stiffness environment is selected by assigning $K_e = 1500$ N/m. Controller parameters are selected as $\Lambda = 2.5I$, $K_V = 150I$, $K_p = 150I$, $\Gamma_\phi = 5$, $\Gamma_F = 5 \times 10^4$, $\Gamma_\Xi = 7 \times 10^{-6}$, and $K_F = 4 \times 10^{-3}$. The results of this simulation are depicted in Figure 6 that demonstrates a satisfactory force tracking convergence in the presence of parametric uncertainty in the second link mass. Moreover, the tracking ability of the proposed system is illustrated in this figure. In addition, estimated compliance converges to its real value, and it makes tracking force control possible.

Simulation 2. Considering the previous case, in this case, a friction model is considered as $F_{sy} = sgn(\dot{y})(1 + 2\dot{y})$ N on the contact surface, to check out the ability of the proposed approach in compensating contact friction during the force control. Figure 7 demonstrates the

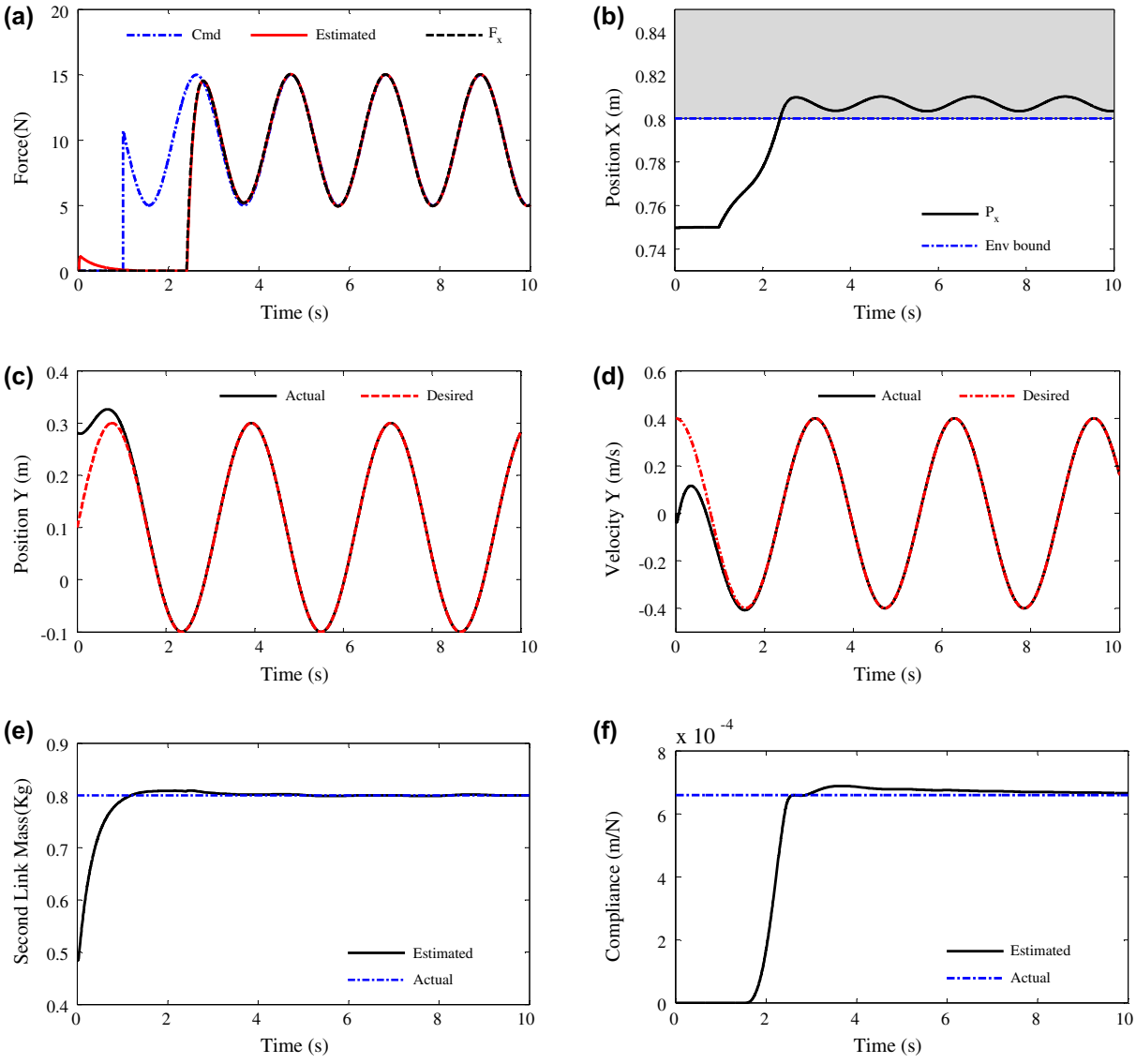

Figure 6. Force control results for $K_e = 1500$ N/m, (a) commanded, estimated, and real end-effector force, (b) end-effector position in x-axis, (c) and (d) commanded and actual trajectory of the end effector in y-axis, (e) second link mass uncertainty and its estimation, and (f) estimated compliance of the environment.

results of this simulation. In fact, the controller estimates force and contact friction simultaneously, and the tracking force control is achieved by accurate estimation of the environment compliance.

Simulation 3. Now, assume that the environment has a higher stiffness. In Figure 8, the manipulator interacts with a higher stiffness environment $K_e = 1.5 \times 10^4$ N/m. In this case, compliance of environment is $\Xi = 6.7 \times 10^{-5}$, and we need to reduce its adaptive gain to $\Gamma_\Xi = 7 \times 10^{-7}$for better convergence. Note that the exact value of the environment compliance is not needed and the adaptive gain can be assigned comparatively. Other parameters remain as in the Simulation 1. Figure 8 illustrates the effectiveness of the proposed method in dealing with the high stiffness environment. Since the environment stiffness is much higher, the end effector remains near the environment boundary and does not enter it like the previous simulations. The faster force convergence and the overshoot of the force control response show the impact of the environment stiffness on the system, which widens the force controller bandwidth. This widening will not cause any serious troubles for the system until the bandwidth of the force controller remains enough far from the bandwidth of the AFE.

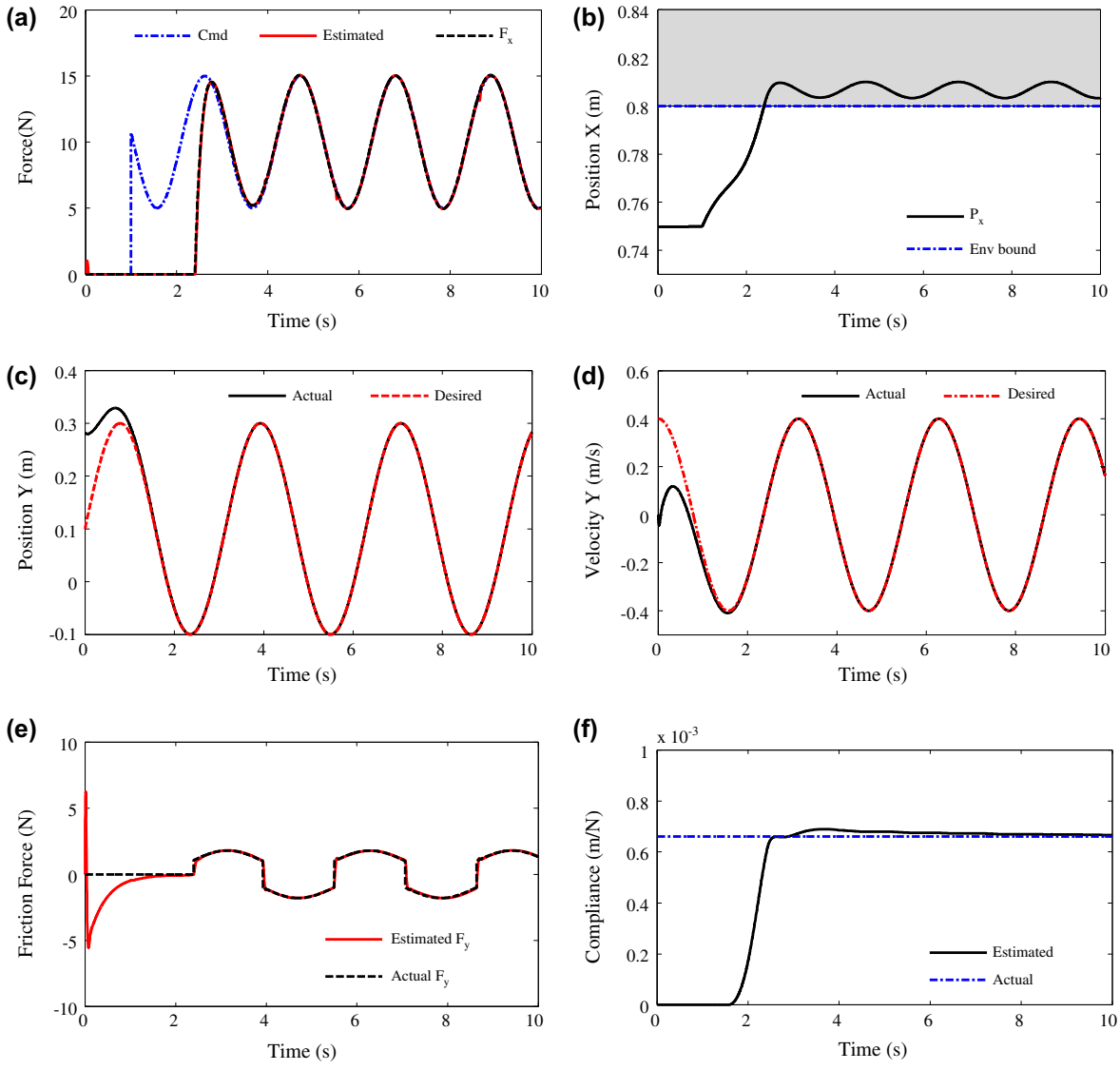

Figure 7. Force control results for $K_e = 1500$ N/m in the presence of contact friction, (a) commanded, estimated, and real end-effector force, (b) end-effector position in x-axis inside the environment, (c) and (d) commanded and actual trajectory of the end effector in y-axis, (e) contact friction, and (f) estimated compliance of the environment.

As it was mentioned before, analyzing the frequency response of the force estimator and the force controller is not possible, since the system is nonlinear and time varying. However, this system can be approximated by a linear system, and this linear system can be used to determine the bandwidth of the system. Before that let us consider some situations which affect the frequency response of the system. Here, high-frequency velocity measurement noise and joint elasticity are added to the robot for more accurate analysis under semi-practical conditions. For this purpose, consider a robot with flexible joints as [34]

$$\begin{aligned} M(q)\ddot{q}+C(q,\dot{q})\dot{q}+G(q)+B(\dot{q})+J(q)^T F+K(q-q_m)=0 \\ I_m\ddot{q}_m+B_m(\dot{q}-\dot{q}_m)+K_m(q-q_m)=\tau \end{aligned} \tag{36}$$

where q_m is the vector of motor angles, I_m is the motor inertia, B_m and K_m are damping and stiffness coefficients of the joints. To see the effects of these unmodeled uncertainties and noise on the controller performance, the previous robot is used for simulation. All the parameters are similar to previous simulations except the estimator coefficient that is $\Gamma_\Xi = 2.5 \times 10^4$ and the environment stiffness that is $K_e = 5.5 \times 10^3$ N/m. Other parameters are selected as $I_m = 1$, $B_m = 100$, $K_m = 300$,

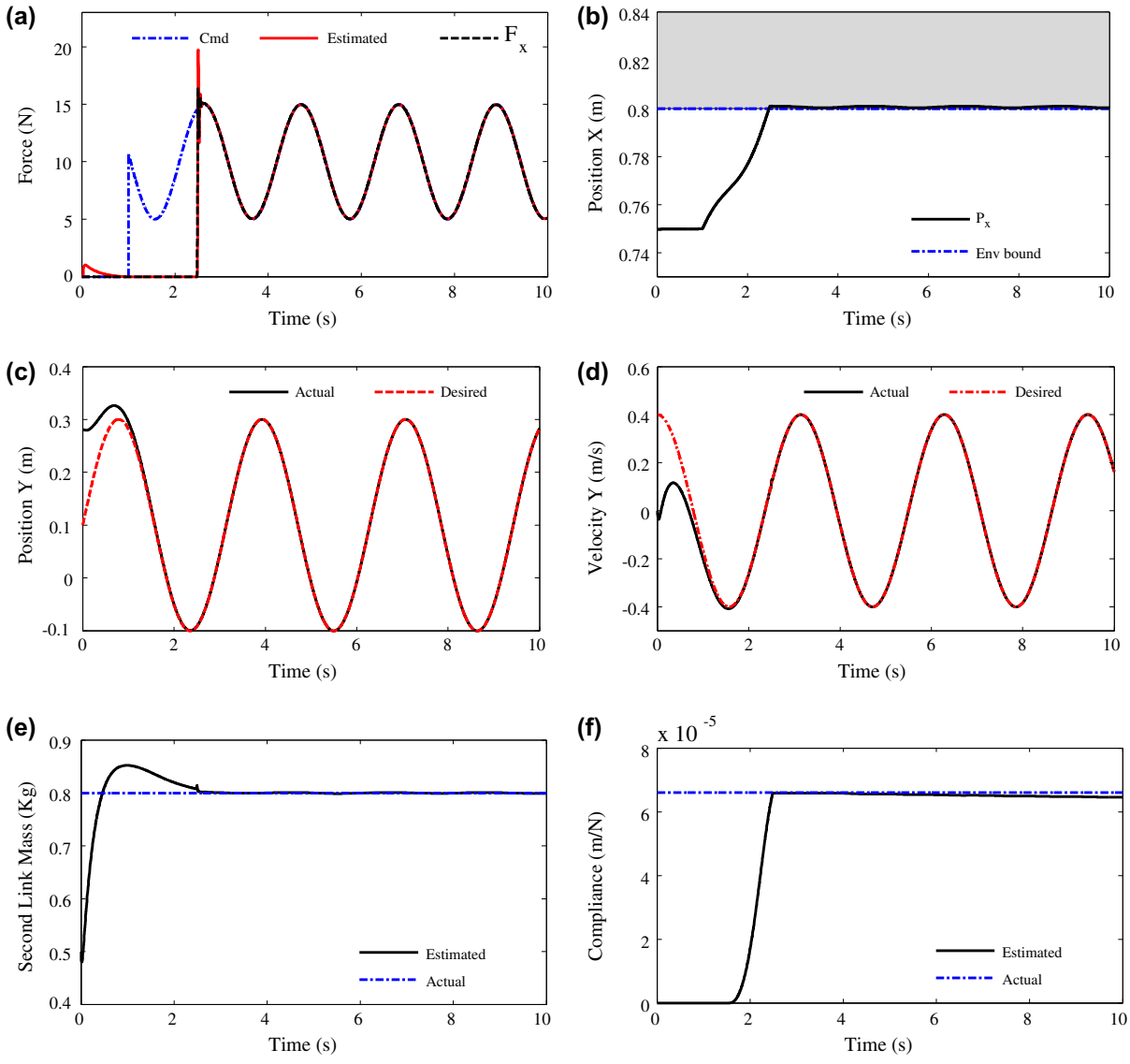

Figure 8. Force control results for $K_e = 1.5 \times 10^4$ N/m, (a) commanded, estimated, and real end-effector force, (b) end-effector position in x-axis, (c) and (d) commanded and actual trajectory of the end-effector in y-axis, (e) second link mass uncertainty and its estimation, and (f) estimated compliance of the environment.

and the noise is a white noise with deviation of 10^{-3} and frequency of 1 kHz. The simulation results are depicted in Figure 9.

Now, for frequency analysis, step response of the AFE is computed by exerting 1 N force on the end effector and recording the estimated force (with no force control loop). For step response of the force controller loop, two different environments are simulated. First one is $K_e = 1.5 \times 10^3$ N/m, and the other is $K_e = 7 \times 10^3$ N/m. The step and frequency responses for them are shown in Figure 10. This figure shows that the bandwidth of the force estimator is 209 rad/s (33.26 Hz), and the bandwidths of force control loops are 6.32 rad/s (1 Hz) and 33.11 rad/s (5.27 Hz) for these two environments, respectively. Note that the changes in the environment are equal to changes in K_F with the same environments. It means that we can increase the bandwidth of the force controller by increasing K_F or even when robot need to interact with a stiffer surface, then K_F can be selected smaller to limit the bandwidth. However, this increasing must be done carefully, since the controller has an admissible response while the estimator has a larger bandwidth rather than the force controller. However, this larger bandwidth of estimator is not always desired and that is because of the existence of the noise that excites the resonance frequencies related to other unmodeled

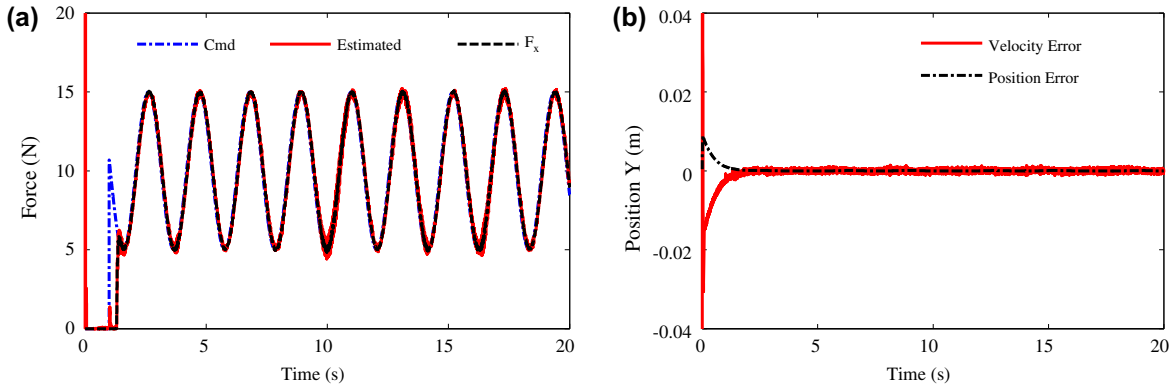

Figure 9. Force control results of the robot with unmodeled joint flexibility and in the presence of measurement noise, (a) commanded, estimated, and real end-effector force, and (b) tracking error of end-effector position in x-axis.

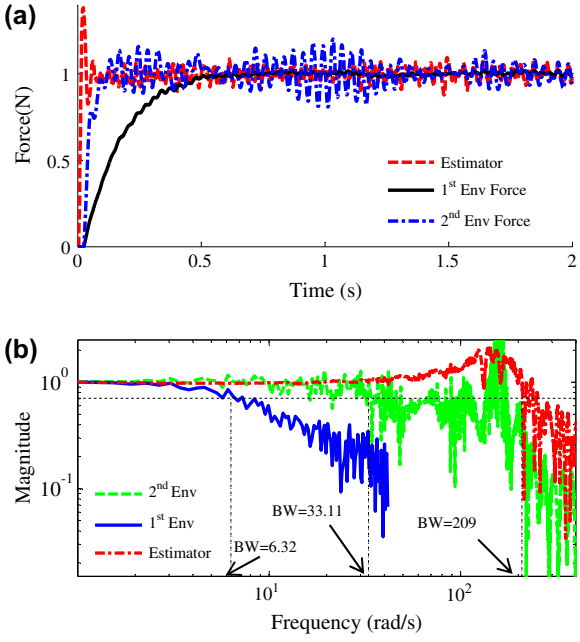

Figure 10. Frequency analysis of the force controller with unmodeled joint flexibility and in the presence of measurement noise using frequency responses of equivalent LTI systems, (a) step responses of the force estimator and the controller for two environments $K_e = 1500\,\mathrm{N/m}$ and $K_e = 7 \times 10^3\,\mathrm{N/m}$ and (b) the frequency response of the equivalent LTI systems which have same step responses with these three-step responses.

dynamics. As it is shown in Figure 10(a), the second force control loop has a resonance inside the force estimation bandwidth, and it is clear that this affects the performance of the controller by some sudden oscillations in its response. Therefore, in the presence of unmodeled dynamics and high-frequency noises, the controller has an effectiveness boundary. Note that this boundary can be extended using other similar methods that are presented for sensor-based methods in the literature.[35–37]

The accuracy of this approach is related to the accuracy of the dynamic model which is provided for the adaptive controller. Definitely, any unmodeled uncertainty with great and non-negligible interfere will affect the force estimation accuracy. However, their models can be added to the controller for compensating them. If the joint elasticity of the robot, stick-slip friction or any other unmodeled uncertainty is not negligible, a new design must be done based on a new dynamic considering these uncertainties, and new adaptive rules are required which consider these uncertainties that are far beyond this article and remain as a future work.

Another simple simulation (without force control loop) was done for a singular trajectory to show the effectiveness of the AFE in estimating the external forces in vicinity of singular points. The trajectory of the robot is selected as $q_d(t) = \left[\frac{\pi}{4} + \frac{\pi}{6}\cos t, -\frac{\pi}{4} - \frac{\pi}{4}\cos t\right]\mathrm{rad}$. First, the disturbance is estimated and then, the external force is computed. Next, the simulation is repeated for estimating the force directly. The results in Figure 11 illustrate significant improvements in dealing with singularity.

Finally, these experiment and simulation results show the efficiency of the proposed sensorless force tracking control in the presence of parametric uncertainty. The frequency analysis of the AFE and the force controller also shows the high capability of AFE in force control applications. However, widening this bandwidth by changing the design or adaptive laws may be valuable for pursuing as future works. In addition, developing AFE for applications in which force measurement is needed, like teleoperations and haptic control, can be considerable.

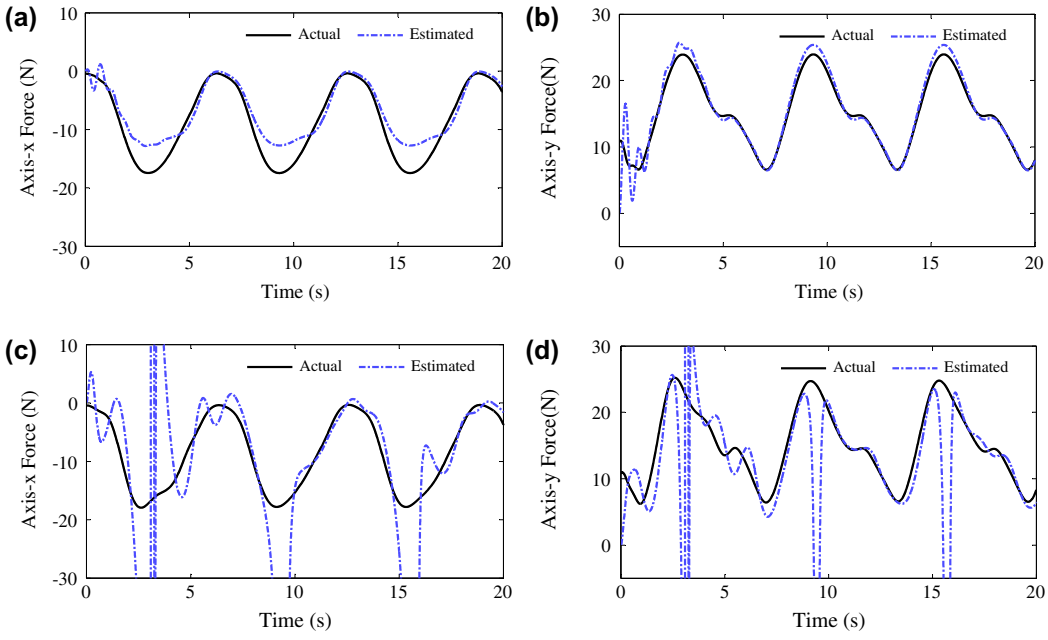

Figure 11. Force estimation results for singular trajectory. (a) and (b) using AFE and (c) and (d) are with disturbance estimation and Jacobian inverse.

6. Conclusion

In this study, a sensorless adaptive hybrid force/position control procedure was presented which used an AFE to estimate the external forces of the manipulator in an inner position/velocity-controlled loop and an outer adaptive force tracking control loop that estimates environment compliance and modifies the trajectory of the manipulator in the force-controlled directions. In fact, this study dealt with three challenging problems: no force sensor was used, environment stiffness was unknown, and some parametric uncertainties existed in the robot model. This approach used a nonlinear-based design that ensures the tracking convergence of force and position in task space and has the rejection ability of the parametric uncertainties in joint space while it is estimating the force. A theorem was presented which guaranteed the asymptotic stability of the system through some conditions. One important condition was the persistency of excitation. Due to difficulty of checking this condition, some considerations were provided to ensure the force estimation convergence. The controller was designed for robots that are in contact with the environment. However, the robot may work in non-contact operation in free space before reaching to the environment, while the adaptive compliance estimator is trying to decrease the fixed force error. A brief study of this condition was described in the study that guaranteed the convergence of the end effector to the environment. Experimental results of a PHANToM Premium robot were provided in a force regulation control while there were several parametric uncertainties in the robot dynamic. Moreover, some simulations were performed for hybrid force/position tracking control of a SCARA manipulator in the presence of parametric uncertainty. In addition to different environments that were simulated, a simulation consisting surface friction was performed to study the performance of the controller in compensating frictions on the end effector. Some frequency analysis was provided at the end that showed a suitable bandwidth of the force estimator which illustrates how the controller parameters and environment stiffness can change the force control bandwidth. Simultaneous convergence of force, uncertainty, and environment compliance indicated the superiority of the proposed controller in dealing with different conditions.

Acknowledgments

The authors would like to express their thanks to Dr Ali Jazayeri for his attempts in preparing the experiment results and also to Dr Mahdi Tavakoli, the director of Telerobotic and Biorobotic Systems (TBS) group at University of Alberta, for providing the experiment facilities for this research.

Notes on contributors

Seyedalimohamad Dehghan received his BS degree in Robotic engineering from Shahrood University of Technology, Shahrood, Iran in 2010. He received his MS degree in control engineering in 2012 from Isfahan University of Technology, Isfahan, Iran. He is currently pursuing his PhD in the Department of Electrical Engineering, University of Isfahan, Iran. During his studies, he participated in several industrial projects including control designing and building several automated machines and robots. His research interests include using different control approaches such as adaptive control, intelligent control, and robust control for non-linear systems especially robots with industrial, rehabilitation, and medical applications and teleoperation systems.

Mohammad Danesh received his BS, MS, and PhD degrees in control engineering in 1997, 1999, and 2007, respectively, all from Isfahan University of Technology (IUT), Isfahan, Iran. Since 2007, he has been with the Department of Mechanical Engineering at IUT. His research interests include robotics, intelligent systems, mechatronics, control of dynamical systems, and stability analysis.

Farid Sheikholeslam received his BS degree in Electronics from Sharif University of Technology, Tehran, Iran in 1990. He received his MS and PhD degrees in Communications and Electrical Engineering from Isfahan University of Technology, Iran, in 1994 and 1998, respectively. Since 1999, he has been with the Department of Electrical and Computer Engineering at Isfahan University of Technology, Iran, where he is a professor of Electrical Engineering. His research interests include control algorithms, stability analysis, nonlinear systems, intelligent control, and robotics.

References

[1] Salisbury JK. Active stiffness control of a manipulator in Cartesian coordinates. In: Proceedings of the 19th IEEE Conference on Decision and Control; 1980; Albuquerque, USA. p. 87–97.

[2] Hogan N. Impedance control: an approach to manipulation: part I – theory. J. Dyn. Syst. Meas. Contr. 1985;107:1–7.

[3] Raibert MH. Hybrid position/force control of manipulators. J. Dyn. Syst. Meas. Contr. 1981;103:126–133.

[4] Mason MT. Compliance and force control for computer controlled manipulators. IEEE Trans. Syst. Man Cybern. 1981;11:418–432.

[5] Vukobratovic M, Tuneski A. Contact control concepts in manipulation robotics-an overview. IEEE Trans. Ind. Electron. 1994;41:12–24.

[6] Yoshikawa T, Sugie T, Tanaka M. Dynamic hybrid position/force control of robot manipulators-controller design and experiment. IEEE J. Rob. Autom. 1988;4:699–705.

[7] Villani L, De Wit CC, Brogliato B. An exponentially stable adaptive control for force and position tracking of robot manipulators. IEEE Trans. Autom. Control. 1999;44:798–802.

[8] Schutter JD, Brussel HV. Compliant robot motion II. A control approach based on external control loops. Int. J. Rob. Res. 1988;7:18–33.

[9] Roy J, Whitcomb LL. Adaptive force control of position/velocity controlled robots: theory and experiment. IEEE J. Rob. Autom. 2002;18:121–137.

[10] Ohnishi K, Shibata M, Murakami T. Motion control for advanced mechatronics. IEEE/ASME Trans. Mechatron. 1996;1:56–67.

[11] Murakami T, Yu F, Ohnishi K. Torque sensorless control in multidegree-of-freedom manipulator. IEEE Trans. Ind. Electron. 1993;40:259–265.

[12] Katsura S, Matsumoto Y, Ohnishi K. Modeling of force sensing and validation of disturbance observer for force control. IEEE Trans. Ind. Electron. 2007;54:530–538.

[13] Eom KS, Suh IH, Chung WK, Sang-rok O. Disturbance observer based force control of robot manipulator without force sensor. In: International Conference on Robotics and Automation; 1998; Leuven, Belgium. p. 3012–3017.

[14] Yajima S, Katsura S. A decoupling controller design and analysis of multilateral control using disturbance observer in modal space. Adv. Rob. 2013;27:71–80.

[15] Santhakumar M. A nonregressor nonlinear disturbance observer-based adaptive control scheme for an underwater manipulator. Adv. Rob. 2013;27:1273–1283.

[16] Kobayashi H, Katsura S, Ohnishi K. An analysis of parameter variations of disturbance observer for motion control. IEEE Trans. Ind. Electron. 2007;54:3413–3421.

[17] Chen W-H, Ballance DJ, Gawthrop PJ, O'Reilly J. A nonlinear disturbance observer for robotic manipulators. IEEE Trans. Ind. Electron. 2000;47:932–938.

[18] Chen X, Komada S, Fukuda T. Design of a nonlinear disturbance observer. IEEE Trans. Ind. Electron. 2000;47:429–437.

[19] Nikoobin A, Haghighi R. Lyapunov-based nonlinear disturbance observer for serial n-link robot manipulators. J. Intell. Rob. Syst.. 2009;55:135–153.

[20] Smith AC, Mobasser F, Hashtrudi-Zaad K. Neural-network-based contact force observers for haptic applications. IEEE Trans. Rob. 2006;22:1163–1175.

[21] Jeong J, Chang P, Park K. Sensorless and modeless estimation of external force using time delay estimation: application to impedance control. J. Mech. Sci. Technol. 2011;25:2051–2059.

[22] Mitsantisuk C, Ohishi K, Urushihara S, Katsura S. Kalman filter-based disturbance observer and its applications to sensorless force control. Adv. Rob. 2011;25:335–353.

[23] Stolt A, Linderoth M, Robertsson A, Johansson R. Force controlled robotic assembly without a force sensor. In: 2012 IEEE International Conference on Robotics and Automation (ICRA); 2012; Saint Paul. p. 1538–1543.

[24] Liu Y-H, Arimoto S, Kitagaki K. Adaptive control for holonomically constrained robots: time-invariant and time-variant cases. IEEE. 1995:905–912.

[25] Su C-Y, Stepanenko Y. Adaptive sliding mode coordinated control of multiple robot arms attached to a constrained object. IEEE Trans. Syst. Man Cybern. 1995;25:871–878.

[26] Kawasaki H, Ueki S, Ito S. Decentralized adaptive coordinated control of multiple robot arms without using a force sensor. Automatica. 2006;42:481–488.
[27] Jung J, Lee J, Huh K. Robust contact force estimation for robot manipulators in three-dimensional space. Proc. Inst. Mech. Eng. Part C: J. Mech. Eng. Sci. 2006;220:1317–1327.
[28] Danesh M, Sheikholeslam F, Keshmiri M. External Force Disturbance Rejection in Robotic Arms: An Adaptive Approach. IEICE Trans. Fundam. Electron. Commun. Comput. Sci. 2005;E88-A:2504–2513.
[29] Danesh M, Sheikholeslam F, Keshmiri M. An Adaptive Manipulator Controller Based on Force and Parameter Estimation. IEICE Trans. Fundam. Electron. Commun. Comput. Sci. 2006;E89-A:2803–2811.
[30] Nakamura Y. Advanced robotics: redundancy and optimization. Boston: Addison-Wesley; 1991.
[31] Chen C-T, Chen C-T. Linear system theory and design. Holt, Rinehart, and Winston: New York (NY); 1984.
[32] Siciliano B. An output feedback parallel force/position regulator for a robot manipulator in contact with a compliant environment. Systems & Control Letters. 1997;29:295–300.
[33] Çavuşoğlu MC, Feygin D, Tendick F. A critical study of the mechanical and electrical properties of the PHANToM haptic interface and improvements for high performance control. Presence: Teleoperators Virtual Environ. 2002;11:555–568.
[34] Goldsmith P, Francis B, Goldenberg A. Stability of hybrid position/force control applied to manipulators with flexible joints. Int. J. Rob. Autom. 1999;14:146–160.
[35] Huang L, Ge S, Lee T. Position/force control of uncertain constrained flexible joint robots. Mechatronics. 2006;16:111–120.
[36] Khorasani K. Adaptive control of flexible-joint robots. IEEE Trans. Rob. Autom. 1992;8:250–267.
[37] Spong MW. Adaptive control of flexible joint manipulators. Syst. Control Lett. 1989;13:15–21.